Chapter 1
Catalytic Chemistry of Hydrocarbon Conversion Reactions on Metallic Single Crystals

Wilfred T. Tysoe

Abstract The ability to be able to follow the chemistry of adsorbates on model catalyst surfaces has, in principle, allowed us to peer inside the "black box" of a catalytic reaction and understand the pathway. Such a strategy is most simply implemented for well-ordered single crystal model catalysts for which the catalytic reaction proceeds in ultrahigh vacuum. Thus, in order to be a good model for the supported catalyst, the single crystal should catalyze the reactions with kinetics identical to those for the supported system. This chapter focuses on catalytic systems that fulfill these criteria, namely alkene and alkyne hydrogenation and acetylene cyclotrimerization on Pd(111). The surface chemistry and geometries of the reactants in ultrahigh vacuum are explored in detail allowing fundamental insights into the catalytic reaction pathways to be obtained.

1.1 Introduction

The role of a heterogeneous catalyst is to open up alternative reaction pathways compared to the corresponding homogeneous-phase reaction, in general, by lowering the reaction activation energy. The ability to follow the chemistry of adsorbates on model catalyst surfaces allows us to peer inside the "black box" of a catalytic reaction and understand the reaction pathway. Accomplishing this relies on being able to study the catalytic reaction chemistry on well-characterized systems that mimic the working catalyst. In general, this implies the model system should catalyze the reaction of interest with kinetics identical to the realistic, often quite complex industrial catalyst. However, it should also ideally be as simple as possible to allow the nature of the catalyst and the reaction pathway to be understood at the molecular level. The simplest, ideal model catalytic systems consist of oriented

W.T. Tysoe (✉)
Department of Chemistry and Biochemistry, University of Wisconsin-Milwaukee, Milwaukee, WI, 53211, USA
e-mail: wtt@uwm.edu

R.M. Rioux (ed.), *Model Systems in Catalysis: Single Crystals to Supported Enzyme Mimics*,
DOI 10.1007/978-0-387-98049-2_1,

single crystal metals that can be studied in ultrahigh vacuum. In addition, the reaction of interest should take place on the model catalyst surface under ultrahigh vacuum conditions so that the full range of surface analytical techniques can be exploited to understand the chemistry. This means that the heat of adsorption of the reactants should be larger than, or at least of the same order as the reaction activation energy. If this condition is not fulfilled, the adsorbates will merely desorb prior to reaction so that little or no information on the surface reaction pathway can be obtained. Under such circumstances, it is necessary to study the reaction under higher pressures.

One area in which such surface science strategies have proved to be remarkably successful in following rather complex surface catalytic reactions has been in the area of hydrocarbon conversion catalysis [1–3], initially focusing on reforming [4–10] and hydrogenation [11, 12] reactions. This work demonstrated, for example, that hydrocarbons could undergo drastic transformations on noble metal surfaces, such as the conversion of ethylene into strongly bound, but relatively unreactive ethylidyne species on Pt(111) [13–23].

Since the intermediates in such hydrocarbon conversion reactions are often present in low coverages or over narrow temperature ranges, strategies have been developed to graft these intermediates onto surface using organic iodide precursors [24–27]. The relative weakness of the carbon–iodine bond compared to the heats of adsorption of the adsorbed hydrocarbon fragment and chemisorbed iodine means that carbon–iodine bond scission is both thermodynamically and kinetically favored compared to other decomposition pathways, thereby allowing hydrocarbon fragments to be relatively cleanly grafted onto transition metal surfaces. This has allowed the properties of these hydrocarbon fragments to be followed providing a fundamental mechanistic understanding of their chemistry and role in the catalytic hydrocarbon conversion pathways. This has also enabled a comparison between the chemistry occurring on extended transition metal surfaces and organometallic compounds [28].

The following describes results of three, relatively simple chemical reactions involving hydrocarbons on model single crystal metal catalysts that illustrate this general approach, namely, acetylene cyclotrimerization and the hydrogenation of acetylene and ethylene, all catalyzed by palladium. The selected reactions fulfill the above conditions since they occur in ultrahigh vacuum, while the measured catalytic reaction kinetics on single crystal surfaces mimic those on realistic supported catalysts. While these are all chemically relatively simple reactions, their apparent simplicity belies rather complex surface chemistry.

The basic hydrogenation pathway for transition metal catalyzed hydrogenation reactions was first described by Horiuti and Polanyi [29, 30] many years ago and was shown to proceed by the metal surface being able to dissociate molecular hydrogen to form the adsorbed hydrogen atoms, which then add in a step-wise fashion to the alkene or alkyne. At the simplest level, therefore, the metal catalyst lowers the reaction activation energy compared to the gas phase by cleaving the relatively strong hydrogen–hydrogen single bond. The true situation, however, turns out to be more complex since at the temperatures at which the catalytic reactions occur

alkenes and alkynes convert to strongly bound species (ethylidyne and vinylidene) that are relatively unreactive, and hydrogenate much more slowly than the rate at which the catalytic reaction occurs. Detailed studies under ultrahigh vacuum conditions allow the reaction pathway to be explored and the roles of these species in the overall catalytic reaction to be identified; to understand, for example, whether they are mere spectators or participate in the reaction, and how their presence affects the overall reaction kinetics. It should, however, be stressed that this is still an ongoing story and even for such simple systems on well-characterized model catalysts there are still gaps in our understanding.

1.2 Chemistry of Acetylene Cyclotrimerization

This direct conversion of acetylene to benzene ($3C_2H_2 \rightarrow C_6H_6$) was first found to be catalyzed by palladium [31–33], although subsequently a wide array of materials was found to catalyze this reaction [34–38]. This reaction fulfills the criteria outlined above since it is catalyzed at high pressures by Pd(111) where benzene is formed from acetylene [39], as well as proceeding in ultrahigh vacuum where the adsorption of acetylene on a palladium surface, particularly Pd(111), yields substantial amounts of benzene [31–33]. Temperature-programmed desorption (TPD) experiments of acetylene on Pd(111) show that benzene is formed in two states at ~280 and ~520 K, where approximately 30% of the adsorbed acetylene is converted to benzene [40]. Studies of benzene itself on Pd(111) show that it desorbs at these temperatures [41] indicating that benzene is rapidly formed from acetylene on Pd(111) and that benzene formation is product-desorption-rate limited. It has been demonstrated that the high-temperature (~520 K) desorption state is due to flat-lying benzene, while the lower-temperature state is due to the presence of tilted benzene formed due to surface crowding [34, 41]; which desorbs at lower temperatures since it is less strongly coordinated to the surface in a tilted orientation than when flat-lying.

The benzene formation rate on Pd(111) under catalytic conditions (i.e., *P*(acetylene) ~20 Torr) is rather insipid with a turnover frequency of ~10^{-2} reactions/site/s [39]. This reaction is first order in acetylene pressure and has a relatively low reaction activation energy of ~2 kcal/mol.

A small amount of C_4 product is also detected in TPD experiments following acetylene adsorption on Pd(111) suggesting benzene is formed in a step-wise fashion on the Pd(111) surface. It was shown, by grafting a C_4H_4 intermediate onto the surface using halogen-containing precursors [42], that the reaction does indeed proceed in a step-wise fashion where two adsorbed acetylene molecules react to form a C_4H_4 intermediate, which has been identified as a tilted metallocyclic species [43]. This finally reacts with a third acetylene molecule, presumably via a Diels–Alder cycloaddition reaction, to form benzene. The ultimate rate of benzene formation in ultrahigh vacuum is limited by the product (benzene) desorption rate rather than the rate of benzene synthesis. A relatively simple geometrical model can

be used to account for the benzene yield as a function of acetylene coverage in TPD assuming that acetylene is immobile on the surface on the time scale of the desorption experiment [40, 44]. This model also accounts for the relative benzene desorption yields from different faces of palladium [33], where the (111) face is more reactive than the (100) and (110) surfaces since the hexagonal Pd(111) surface correctly orients the acetylene to form benzene [45]. Larger benzene formation yields have been found using laser-induced thermal desorption where the bulk sample heating rate is much slower (product desorption is induced by a very fast heating of a local region), presumably forming more benzene by allowing some surface mobility [46–48] and the catalytic act has been observed directly using scanning tunneling microscopy [49].

Thus, surface analytical experiments have been able to successfully identify the benzene cyclotrimerization pathway and the nature of the reaction intermediates in ultrahigh vacuum. The question, however, remains whether this pathway also operates at higher pressures. The observation that reaction occurs rapidly in ultrahigh vacuum would imply that the catalytic reaction under high pressures should be fast, while relatively insipid rates are measured experimentally [39]. Measurements of the benzene formation rate as a function of time using an initially clean, supported palladium catalyst reveal that a high initial cyclotrimerization rate decreases to a low steady-state rate as a function of time on stream [50]. Molecular beam results on clean palladium in ultrahigh vacuum reveal a similar phenomenon. This self-poisoning effect is attributed to the formation of stable vinylidene species (CH_2=C=) that are detected in surface science experiments when a Pd(111) surface is exposed to acetylene at room temperature [51], and these react to form neither ethylene nor benzene, at least in TPD experiments on vinylidene-covered Pd(111) in ultrahigh vacuum [52].

In order to further explore the role of vinylidene species, the structures of the surface species formed from acetylene on palladium were investigated. At low temperatures, low-energy electron diffraction intensity versus beam energy (LEED I/E) experiments reveal that acetylene adsorbs with the carbon–carbon bond close to parallel to the surface on the hexagonal close-packed (hcp) hollow site, with a bond length of ~1.36 Å [53] and is therefore ~sp^2 hybridized. This structure is in good agreement with theoretical calculations [54]. Acetylene exhibits a well-defined $\sqrt{3} \times \sqrt{3}$ R30° LEED pattern at a coverage of 0.33 monolayers (where, in the following, coverages are referenced to the atom site density on the Pd(111) surface) and the saturation coverage is somewhat higher at ~0.45 ML.

At room temperature and above, where the catalytic reaction is carried out, acetylene is converted into a vinylidene species [51]. The structure of vinylidene, again determined from LEED I/E measurements, is depicted in Fig. 1.1.

It bonds with the C=C bond tilted somewhat with respect to the surface normal and the measured structure is in accordance with that calculated using density functional theory [55, 56]. The saturation coverage of vinylidene at ~300 K is ~1 ML. Furthermore, a vinylidene overlayer is found on the surface during palladium-catalyzed reactions of acetylene [13], which suggests that acetylene cyclotrimerization proceeds in the presence of a vinylidene-covered surface, rather

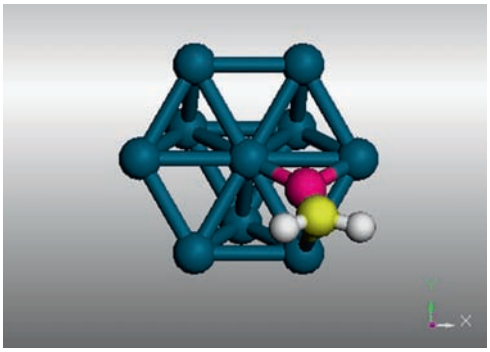

Fig. 1.1 Depiction of the structure of vinylidene species on Pd(111)

than on clean Pd(111). Analogously, strongly bound ethylidyne species are found on ethylene hydrogenation catalysts (see below), and it has been suggested that alkenes can still access the catalyst surface at sufficiently high pressures in spite of the presence of ethylidyne species [14–19], implying these surface layers are sufficiently flexible or mobile to accommodate additional species [57]. High-pressure CO adsorption was used to further explore this notion on vinylidene-covered Pd(111) [58]. A vinylidene-covered surface was pressurized with carbon monoxide and investigated using reflection-absorption infrared spectroscopy (RAIRS) to monitor the coverage of carbon monoxide on the surface. Figure 1.2 plots the adsorbed CO stretching mode intensity (at ~1800 cm^{-1}) as a function of pressure on vinylidene-covered Pd(111).

The CO vibrational frequency indicates that CO adsorbs on the metal surface in spite of the presence of a vinylidene overlayer. Clearly, additional CO adsorbs onto the vinylidene-covered surface at sufficiently high pressures (several Torr). Adsorption is completely reversible and a Langmuir isotherm plotted with the data is shown (Fig. 1.2). Measurement of the variation in initial CO coverage with pressure as a function of temperature reveals that the heat of adsorption of CO on vinylidene-covered Pd(111) is 8 ± 1 kcal/mol, significantly lower than the value of ~35 kcal/mol measured for CO on clean Pd(111) in ultrahigh vacuum [59, 60]. Since carbon monoxide adsorbs onto the palladium surface, the strength of the CO–Pd bond should be ~35 kcal/mol, and the lower value on the vinylidene-covered surface is presumably due to the additional work required to create room for the carbon monoxide. The CO coverage is calibrated from the change in infrared absorbance of CO on Pd(111) as a function of coverage at low coverage. It should be noted that infrared absorbances are often not reliable measures of coverage due to dipole–dipole coupling effects [61] but this is likely to be less of a problem at low coverage.

These results suggest that acetylene should also adsorb onto palladium in the presence of a vinylidene monolayer at sufficiently high pressures. As noted above, surface science experiments conclude that benzene is formed from acetylene on Pd(111) under UHV conditions by an initial reaction between two acetylene molecules to form a C_4H_4 intermediate [42, 43], followed by reaction with a third acety-

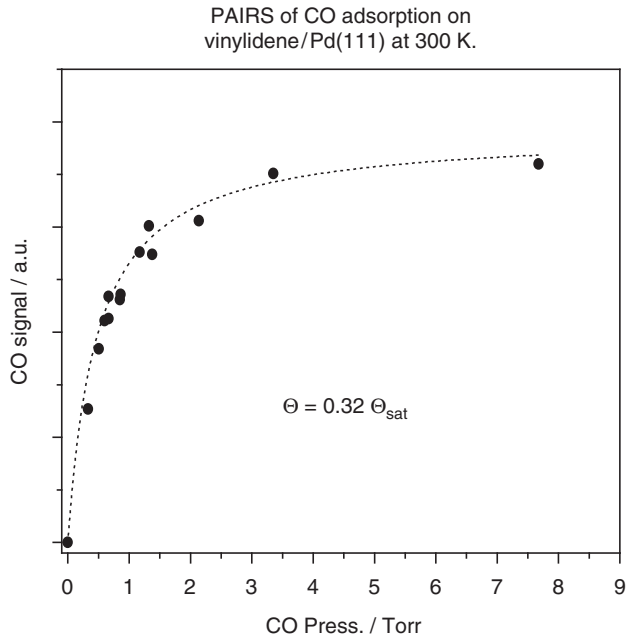

Fig. 1.2 Adsorption isotherm for CO on a vinylidene-saturated surface collected at a sample temperature of 300 K. The saturation coverage calculated from the integrated absorbance of CO on the clean surface is estimated to be ~32% of that which can be accommodated on clean Pd(111). The line plotted through the data is a Langmuir isotherm. (Reproduced with permission from [58]. Copyright 2001, American Institute of Physics.)

lene molecule to yield benzene in a step-wise fashion. This reaction requires a relatively large ensemble of atoms on the surface [62, 63]. While it is feasible that a single acetylene molecule could adsorb onto a vinylidene-covered surface, it is not likely to accommodate such large ensembles. However, reaction between acetylene and vinylidene to form a metallocycle has been observed in organometallic molecules [64–66]. It is therefore possible that adsorbed acetylene could react with adsorbed vinylidene on Pd(111) under high-pressure conditions to form benzene. If this proposal is true, gas-phase acetylene and adsorbed vinylidene should react *at the same rate* at which benzene is synthesized catalytically. This postulate was tested by forming a ^{13}C-labeled vinylidene layer and reacting it with ^{12}C-labeled acetylene and following the change in the coverage of labeled vinylidene on the surface as a function of time. Nuclear magnetic resonance (NMR) is selected to follow this reaction since ^{12}C is NMR invisible, while ^{13}C can easily be detected [67]. Unfortunately, NMR is not sufficiently sensitive to detect adsorbates on single crystal surfaces, so this experiment was carried out using alumina-supported palladium to increase the surface area. Infrared spectroscopy was used to confirm that vinylidene species are formed on Pd/Al_2O_3 [68] since the CH_2 bending mode is detected both on Pd(111)

and Pd/Al_2O_3 following acetylene adsorption at 300 K confirming that vinylidene is also deposited onto the high-surface-area sample. The assignment to a CH_2 (rather than a C=C) mode was confirmed using ^{13}C-labeled acetylene where only a small shift in vibrational frequency was found. However, such as small shift precludes infrared spectroscopy being used to follow ^{13}C-vinylidene replacement [20, 21]. The infrared spectra collected following adsorption of ethylene onto Pd(111) and Pd/Al_2O_3 at room temperature were also compared and both display an intense methyl bending mode at 1329 cm^{-1} and a weaker C–C stretching mode at 1098 cm^{-1} [22, 23], confirming that ethylidyne (CH_3–C≡) species are also formed from ethylene on both the surfaces. This will be discussed in greater detail below. These results imply that the surface chemistry of Pd/Al_2O_3 strongly resembles that found on Pd(111) in accordance with the observation that both Pd(111) and supported palladium catalyze hydrogenation reactions with identical kinetics.

An alumina-supported palladium sample was exposed to $^{13}C_2H_2$ to form a ^{13}C-labeled vinylidene monolayer and the resulting NMR signal collected. The sample was then exposed to $^{12}C_2H_2$. The experimentally determined benzene formation rate measured at 300 K [39] suggests that exposing vinylidene to 345 Torr of acetylene for 130 s should remove ~63% of it. The NMR spectra resulting from this experiment are shown in Fig. 1.3 and reveal that surface species are removed by reaction with gas-phase ^{12}C-acetylene at the same rate at which the reaction proceeds [68]. This is indicated by the vertical lines in Fig. 1.3, which represent the integrated areas under the NMR spectra, and considered to be proportional to the coverage of ^{13}C-labeled vinylidene. The line labeled A_0(exp) indicates the initial ^{13}C-labeled vinylidene ($^{13}CH_2$=^{13}C=) coverage (spectrum 1.3a), the line labeled A_t(calc) is 37% of A_0(exp) – the amount expected to remain after reaction with $^{12}C_2H_2$ and calculated as described above – and A_t(exp) represents the amount found experimentally from spectrum 1.3b. These values are clearly in good agreement. The resulting product gas mixture was analyzed by mass spectroscopy and the mass spectrum of the benzene formed during this experiment is shown as an inset, which shows a peak at 80 amu confirming the ^{13}C-labeled vinylidene initially present on the surface has undergone reaction to form benzene. These results clearly indicate that adsorbed vinylidene species, although unreactive in ultrahigh vacuum [52], are rendered labile under high gas pressures. This high-pressure reaction pathway is summarized in Scheme 1.1.

There are two routes by which benzene can form from acetylene on Pd(111). The first found under UHV conditions occurs by a pathway in which benzene is produced via a C_4H_4 intermediate formed from two adsorbed acetylenes, that rapidly reacts with a third acetylene to form benzene. An alternative, but much slower reaction occurs between vinylidene and acetylene to form the C_4H_4 intermediate as shown in Scheme 1.1. The existence of two distinct pathways accounts for the decrease in activity of the high-surface-area catalysts as a function of time on stream [50]. Reaction initially occurs on the clean surface by the first pathway to rapidly form benzene. However, vinylidene species accumulate on the surface so that reaction then proceeds by the slower pathway depicted in Scheme 1.1.

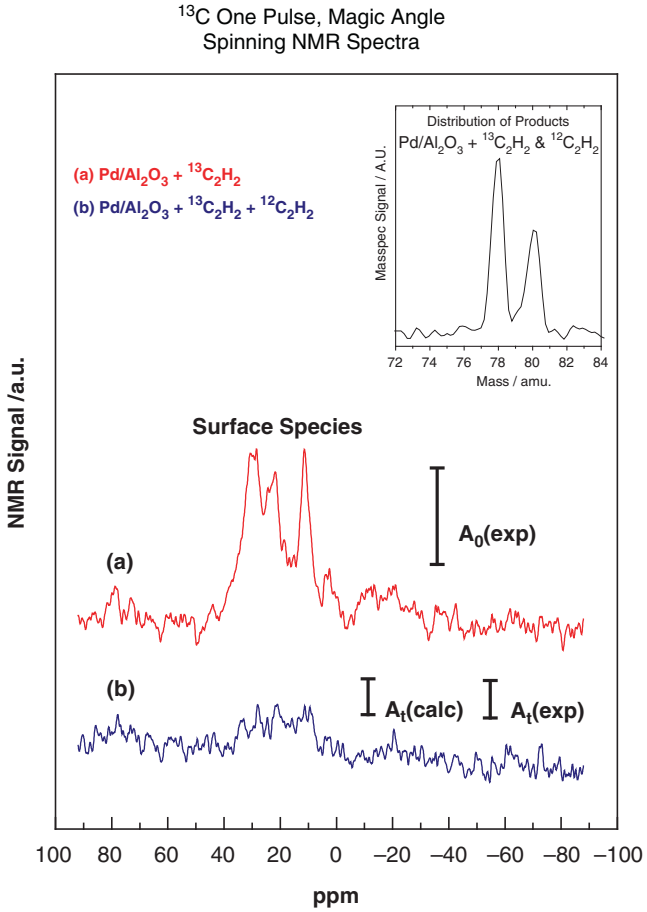

Fig. 1.3 ^{13}C-magic-angle spinning NMR spectra of vinylidene formed on alumina-supported palladium (**a**), and after exposure to $^{12}C_2H_2$ (345 Torr, 130 s). Shown as an *inset* is a mass spectrum of the benzene that is formed. (With kind permission from Springer Science and Business Media.)

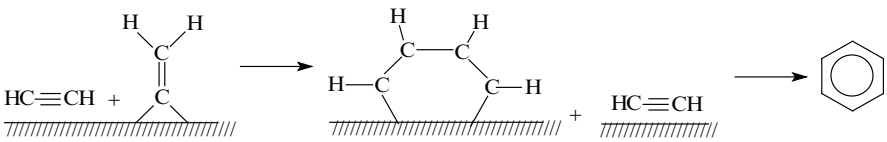

Scheme 1.1 Proposed benzene formation pathway for acetylene under catalytic conditions

1.3 Effect of Hydrogen Addition on the Benzene Formation Rate

The effect of hydrogen on the Pd(111)-catalyzed rate of benzene formation was also explored to provide insights into acetylene hydrogenation since, as shown below, Pd(111) catalyzes acetylene hydrogenation. It would thus be expected a priori that hydrogen addition should result in a decrease in the benzene formation rate since acetylene is being removed from the surface. In contrast, as shown in Fig. 1.4, the benzene formation rate increases substantially when hydrogen is added to the reaction mixture.

As noted above, the Pd(111) model catalyst is covered by vinylidene species during cyclotrimerization catalysis in the presence of acetylene alone. An infrared interrogation of a Pd(111) model catalyst during *acetylene* hydrogenation reveals the presence of some ethylidyne in addition to vinylidene. This suggests that

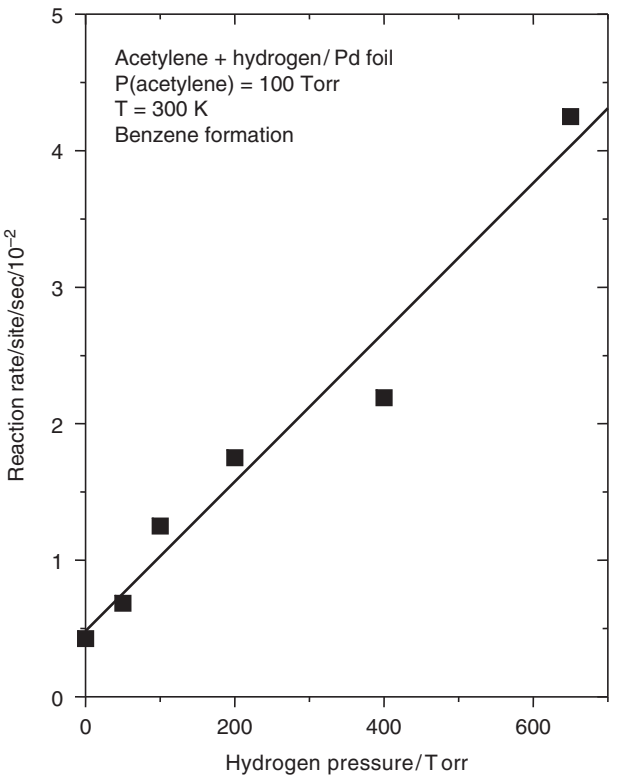

Fig. 1.4 Plot of the benzene formation rate as a function of hydrogen pressure catalyzed by Pd(111). (With kind permission from Springer Science and Business Media.)

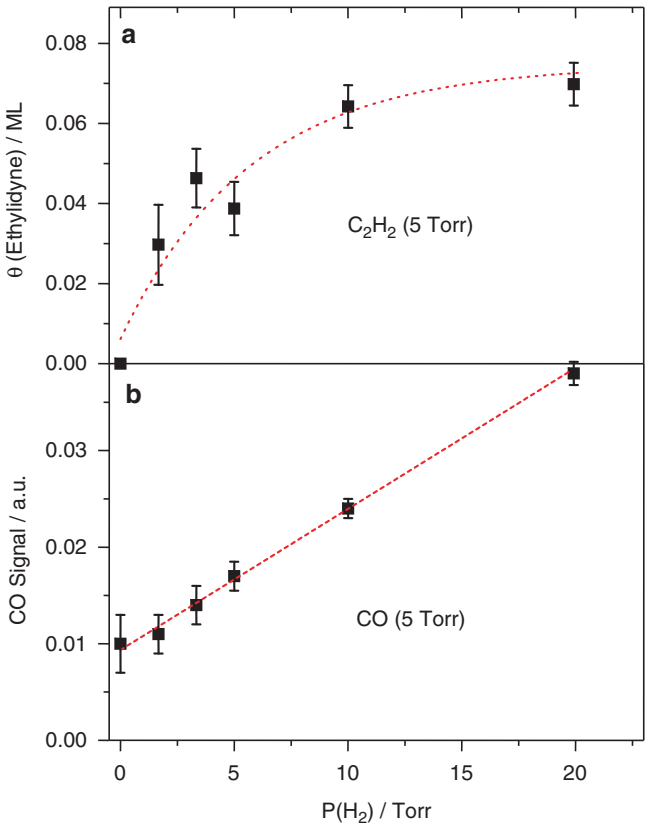

Fig. 1.5 (**a**) The ethylidyne coverage at 300 K as a function of hydrogen pressure in the presence of 5 Torr of acetylene, (**b**) the CO coverage on the surface following reaction. (With kind permission from Springer Science and Business Media.)

adsorbed vinylidene species can react with hydrogen to form ethylidyne. Ethylidyne species will be discussed in greater detail below, but they can be identified by infrared spectroscopy from an intense vibrational mode at ~1329 cm^{-1} [22, 23]. Displayed in Fig. 1.5a is the intensity of the ~1329 cm^{-1} (ethylidyne) mode on Pd(111) as a function of hydrogen pressure for the reaction of hydrogen with 5 Torr of acetylene.

In the absence of hydrogen, the surface is completely covered by vinylidene species (Fig. 1.1) while with increasing hydrogen a larger proportion of the surface becomes covered by ethylidyne species and the ethylidyne coverage reaches a maximum at a hydrogen pressure of ~15 Torr. Note, however, that the coverage does not attain the saturation coverage found on clean Pd(111) ($\Theta_{sat} = 0.25$) so the surface is covered by a mixture of ethylidyne and vinylidene moieties. As noted above (Fig. 1.2), carbon monoxide can adsorb onto a vinylidene-saturated surface at high pressures. However, the increased ethylidyne coverage provides a more

open surface and allows more carbon monoxide to adsorb onto the surface (see Fig. 1.5b). This hints at the true complexity of an apparently simple hydrogenation reaction, arising from the presence of strongly bound carbonaceous species on the surface. The implications of this on the hydrogenation kinetics will be explored below.

This chemistry was investigated further by measuring the kinetics of vinylidene reaction with hydrogen using infrared spectroscopy. In this case, a saturated vinylidene overlayer is allowed to react with high pressures of hydrogen. The formation of ethylidyne species is found, and the time variation in the ethylidyne coverage, measured from the intensity of the ethylidyne infrared signal, is plotted in Fig. 1.6 using a hydrogen pressure of 0.1 Torr, which shows the ethylidyne coverage initially increases, attains a maximum, and then decreases. Performing a similar experiment for an initially ethylidyne-covered surface shows that this is also removed by reaction with high pressures of hydrogen [69]. The data presented in Fig. 1.6 therefore represent a reaction in which there is an initial conversion of vinylidene to ethylidyne, causing an increase in ethylidyne coverage which is then titrated from the surface by hydrogen causing the signal to decrease as depicted in Scheme 1.2.

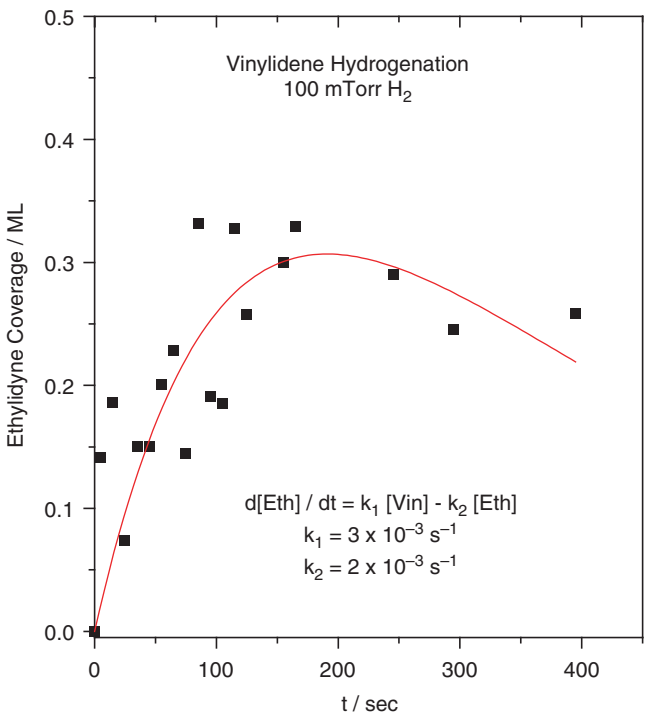

Fig. 1.6 Plot of ethylidyne coverage versus time from reaction of a vinylidene-covered Pd(111) surface with hydrogen, where d[Eth]/d*t* is the rate of change of ethylidyne coverage. (Reproduced from [102] with permission from Elsevier.)

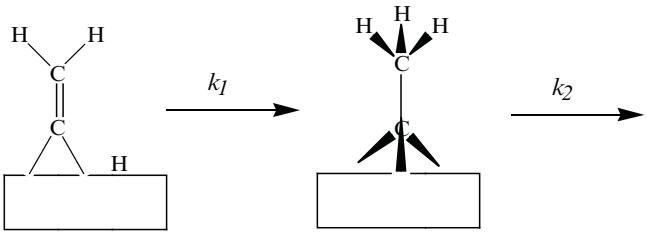

Scheme 1.2 Proposed reaction pathway between vinylidene and hydrogen to form ethylidyne

The kinetic equations for this simple sequential reaction can be solved analytically and the rate depends on two rate constants, k_1 and k_2 (see Scheme 1.2). The value of k_2 is measured independently by similarly monitoring the time dependence of the intensity of the ethylidyne infrared signal of an initially ethylidyne-covered surface in the presence of hydrogen using infrared spectroscopy [69].

The results of this experiment are shown in Fig. 1.7, which displays the plots of the rate constants for ethylidyne removal from both clean Pd(111) (▲) and alumina-supported palladium (■) as a function of hydrogen pressure. The values for these two samples are in good agreement, in accordance with the observation that a Pd(111) single crystal is a good model for the supported hydrogenation catalyst (see below).

This reveals the reaction rate is first order in hydrogen pressure and the implications of this on the overall reaction kinetics will be explored below. Since k_2 is known, the kinetic data shown in Fig. 1.6 can then be fit into a single parameter (k_1) and the fit is shown as a solid line. The resulting value of k_1, the rate constant for the conversion of vinylidene to ethylidyne, also varies with hydrogen pressure and its dependence is shown in Fig. 1.8, which also exhibits a first-order hydrogen pressure dependence. It is interesting to note that the rate constant for ethylidyne removal ($k_1 = 3.1 \pm 0.3 \times 10^{-2}\ P(H_2)\ s^{-1}$, Fig. 1.8) is very close to that for vinylidene-to-ethylidyne conversion ($k_2 = 3.2 \pm 0.5 \times 10^{-2}\ P(H_2)\ s^{-1}$, Fig. 1.7). The vinylidene saturation coverage (Θ_{sat}(vinylidene) = 1.0 ML [51]) is larger of ethylidyne (Θ_{sat}(ethylidyne) = 0.25 ML [14, 15]) so the picture is more complicated than depicted in Scheme 1.2. This may mean the conversion of vinylidene to ethylidyne is limited by the removal rate of vinylidene to make space on the surface to accommodate the ethylidyne.

These results indicate that the origin of the acceleration in the rate of acetylene cyclotrimerization due to the addition of hydrogen measured above (Fig. 1.4) arises from a combination of the formation of a more open ethylidyne-covered surface, and possibly also the removal of the ethylidyne once it has been formed to produce regions of relatively clean palladium.

It is evident that acetylene cyclotrimerizes rapidly on clean Pd(111) as described above. This, therefore, raises the question whether acetylene cyclotrimerization reactions can also occur on the ethylidyne-covered portion also. This is addressed

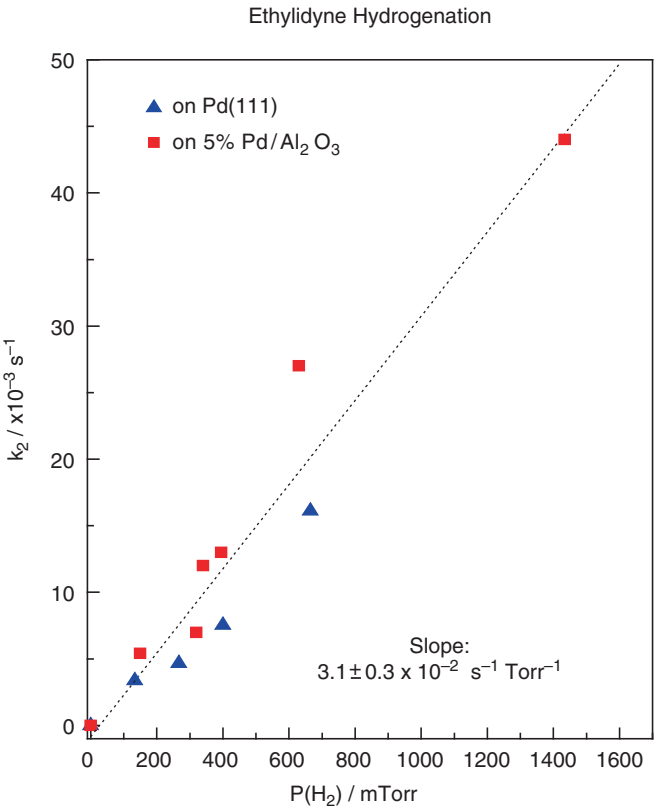

Fig. 1.7 Plot of the rate constant (k_2) for ethylidyne hydrogenation on Pd(111) as a function of hydrogen pressure (Reproduced from [102] with permission from Elsevier.)

by the data shown in Fig. 1.9, which displays TPD data for hydrogen and benzene desorption following exposure of acetylene to clean and ethylidyne-saturated Pd(111).

The top spectra show the hydrogen desorption profiles for acetylene adsorbed on clean and ethylidyne-saturated Pd(111). These spectra are typical for the thermal decomposition of ethylidyne and vinylidene species indicating that both are thermally stable at well above 400 K. More important are the bottom benzene (78 amu) desorption spectra. The top spectrum, collected following acetylene adsorption on clean Pd(111) shows the two peaks due to flat-lying (at ~520 K) and tilted (~280 K) benzene discussed above. The bottom spectrum shows a strong benzene desorption signal, indicating that acetylene cyclotrimerizes to benzene both on clean and ethylidyne-saturated surfaces. Interestingly, the spectrum for desorption from ethylidyne-saturated Pd(111) exhibits only a single peak due to the desorption of tilted benzene. Evidently, the crowding due to the presence of a saturated ethylidyne overlayer precludes the formation of flat-lying benzene and forms benzene at a lower temperature than on the clean surface.

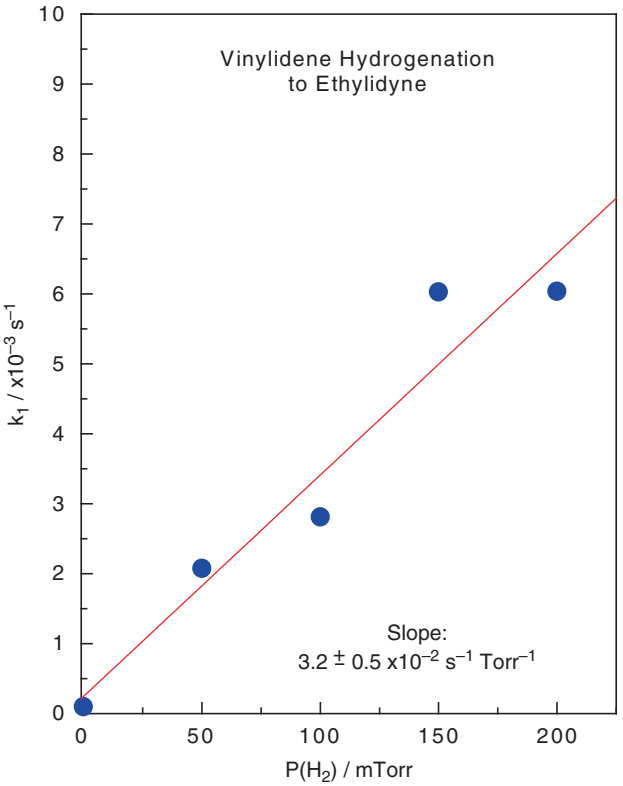

Fig. 1.8 Plot of rate constant (k_1) for vinylidene conversion to ethylidyne on Pd(111) as a function of hydrogen pressure. (Reproduced from [102] with permission from Elsevier.)

The picture that emerges is one in which the nature of the strongly bound carbonaceous overlayer controls the catalytic reaction pathway. In the absence of hydrogen, the benzene formation rate is relatively low since the surface rapidly becomes covered by vinylidene species (Fig. 1.1) so that benzene is formed slowly by a reaction between vinylidene species and acetylene that adsorbs at high pressures between the vinylidenes (Scheme 1.1). When hydrogen is added to the reaction mixture, in addition to hydrogenating acetylene to ethylene, hydrogen can also react with vinylidenes to form ethylidynes and these may also be titrated from the surface, thereby creating a more open surface, which allows sufficiently large ensembles to be created so that benzene is now able to form more rapidly by reaction between adsorbed acetylenes via the pathway found under ultrahigh vacuum conditions. In catalytic parlance, this would be identified with the presence of two types of "active sites," one of which is created by hydrogen addition.

It should be emphasized that the proportion of benzene formed in the reaction is much lower than the yield of ethylene formed by acetylene hydrogenation.

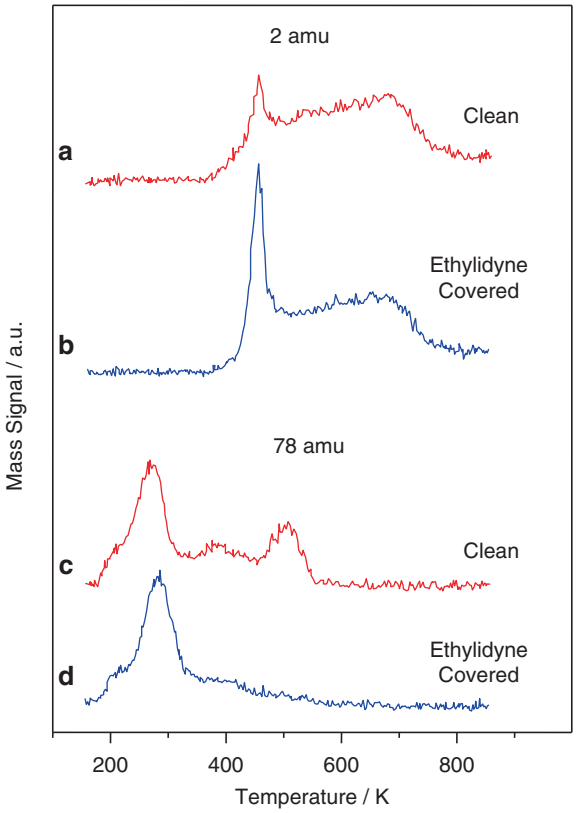

Fig. 1.9 Temperature-programmed desorption (TPD) of (**a**) hydrogen and (**c**) benzene from acetylene on clean Pd(111) compared with the spectra for (**b**) hydrogen and (**d**) benzene from ethylidyne-covered Pd(111). (With kind permission from Springer Science and Business Media.)

However, measuring the hydrogen pressure dependence of a reaction that does not involve hydrogen (acetylene cyclotrimerization) enables these effects to be disentangled in a way that would not be easily possible by studying the hydrogenation reaction alone. These results set the stage for understanding the catalytic hydrogenation of alkenes and alkynes and establishing the effect of the presence of ethylidyne and vinylidene on the hydrogenation kinetics.

1.4 Alkene and Alkyne Hydrogenation

These are classical catalytic reactions and have been the subject of fundamental study for many years [70–80]. Most transition metals catalyze hydrogenation reactions to a greater or lesser extent and the reaction kinetics for all of these are

remarkably similar showing a positive order in hydrogen pressure between about 0.8 and 1.4, depending on the reaction conditions, and a generally zero or negative dependence on hydrocarbon pressure, indicating that hydrogen adsorption is blocked by the hydrocarbon [79]. Activation energies for the reaction are also remarkably constant, typically being between about 8 and 11 kcal/mol, and the reaction is not structure sensitive. Fundamental studies of ethylene hydrogenation catalyzed by a Pt(111) model single crystal [12] using a high-pressure reactor incorporated into an ultrahigh vacuum system revealed a surface covered by ethylidyne species after reaction [14, 15]. Sum-frequency generation [16–19] and infrared [20–23] experiments demonstrate that these are present *during* reaction. Such carbonaceous layers have subsequently been found to be rather ubiquitous, with only the nature of the hydrocarbon species varying with the type of catalyst and reactant. Thus, as shown above for example, acetylene forms vinylidene following adsorption on Pd(111) at ~300 K [13] and relatively thick carbonaceous layers are found on molybdenum following catalysis [81–83].

1.4.1 Acetylene Hydrogenation

This reaction is of particular interest since palladium is capable of selectively hydrogenating acetylene to ethylene in the presence of excess ethylene and is used to provide pure ethylene feedstocks for subsequent polymerization reactions [84]. Insights into the nature of the surface during reaction with acetylene and hydrogen described above are used as a basis for understanding the hydrogenation catalysis.

Acetylene is rehybridized following adsorption on clean Pd(111) at low temperatures, and is oriented with the carbon–carbon axis parallel to the surface. TPD experiments of acetylene on hydrogen-covered Pd(111) [85] still reveal the formation of benzene, but with a lower yield than from the clean surface. Some butene is formed at ~300 K due to hydrogenation of the C_4 metallocycle providing further confirmation of its participation in the benzene formation pathway. In addition, a relatively intense ethylene feature appears at ~280 K, due to acetylene hydrogenation, where the hydrogenation rate is first order in hydrogen coverage. Assuming that hydrogenation occurs via a step-wise (Horiuti–Polanyi [29, 30]) pathway, the reaction must proceed via a vinyl intermediate. This can be grafted onto Pd(111) using vinyl iodide, where the vinyl species hydrogenate more rapidly than adsorbed acetylene indicating that the rate-limiting step is the addition of hydrogen to acetylene to form the vinyl intermediate [86].

The rate of acetylene hydrogenation on a clean Pd(111) model catalyst has been measured using a high-pressure reactor incorporated in an ultrahigh vacuum chamber [87]. This allows the reaction to be carried out on clean, well-characterized samples. This yields a kinetic rate equation (in units of reactions/site/s) of the form:

$$\text{Rate} = 5 \pm 1 \times 10^{6} P\left(\text{H}_2\right)^{1.04 \pm 0.02} P\left(\text{C}_2\text{H}_2\right)^{-0.66 \pm 0.02} \exp\left(-9600 \pm 200 / RT\right) \quad (1.1)$$

where a site is taken to be an exposed palladium atom on a (111) surface [88]. Reaction proceeds with an activation energy of 9.6 ± 0.2 kcal/mol when using hydrogen and 9.1 ± 0.1 kcal/mol when using deuterium; consistent with hydrogen addition being involved in the rate-limiting step. The measured reaction kinetics are typical for transition metal catalyzed hydrogenation reactions, which have reaction activation energies ~10 kcal/mol, a zero or negative order in hydrocarbon pressure and some positive order between ~1.0 and ~1.5 in hydrogen pressure. These values are also in very good agreement with kinetic data collected for other supported palladium catalysts [74, 77, 89–99], confirming that palladium provides a good model for a supported acetylene hydrogenation catalyst. Clearly, the reaction kinetics are more complex than can be accounted for by a simple Horiuti–Polanyi pathway [29, 30], where the reaction rate is proportional to hydrogen coverage and would therefore yield a hydrogen pressure dependence substantially lower than unity. Evidently, the change in the nature of the carbonaceous layers on the surface, identified above, will affect the overall reaction kinetics. This is illustrated in the following by investigating the hydrogen pressure dependence of palladium-catalyzed acetylene hydrogenation.

The proportion of the surface covered by ethylidyne or vinylidene species, depends on the hydrogen pressure due to the reactions depicted in Scheme 1.2. Both the coverage of carbon monoxide (Fig. 1.5b) and the rate of acetylene cyclotrimerization (Fig. 1.4) vary linearly with hydrogen pressure, as a result of the first-order hydrogen pressure dependence of vinylidene-to-ethylidyne conversion (Fig. 1.8) and ethylidyne titration from the surface (Fig. 1.7). This suggests that the number of "surface sites" N_S available for reaction varies with hydrogen pressure, $P(\text{H}_2)$ and can be expressed as:

$$N_S = A + BP(\text{H}_2) \quad (1.2)$$

The parameter A represents the number of "sites" available at very low hydrogen pressures corresponding to the intercepts in Figs. 1.4 and 1.5b due to adsorption on a vinylidene-saturated surface. The parameter B represents the additional "sites" that are made available by reaction with hydrogen to form the more open vinylidene + ethylidyne-covered surface, exemplified by the slopes of Figs. 1.4 and 1.5b. Clearly, the acetylene coverage depends on its pressure so that A and B will also depend on acetylene pressure.

Assuming hydrogen dissociatively adsorbs on the surface and that the reaction rate is proportional to the hydrogen atom coverage as suggested by surface science experiments, the hydrogen pressure dependence of the acetylene hydrogenation rate can be expressed as:

$$\text{Rate} \propto \sqrt{P(\text{H}_2)} \times (1 + \gamma P(\text{H}_2)) \quad (1.3)$$

where $\gamma = B/A$ so that for $\gamma = 0$, the reaction order is 0.5, and for very large values of γ the reaction order tends to 1.5. These results also suggest that since B depends on

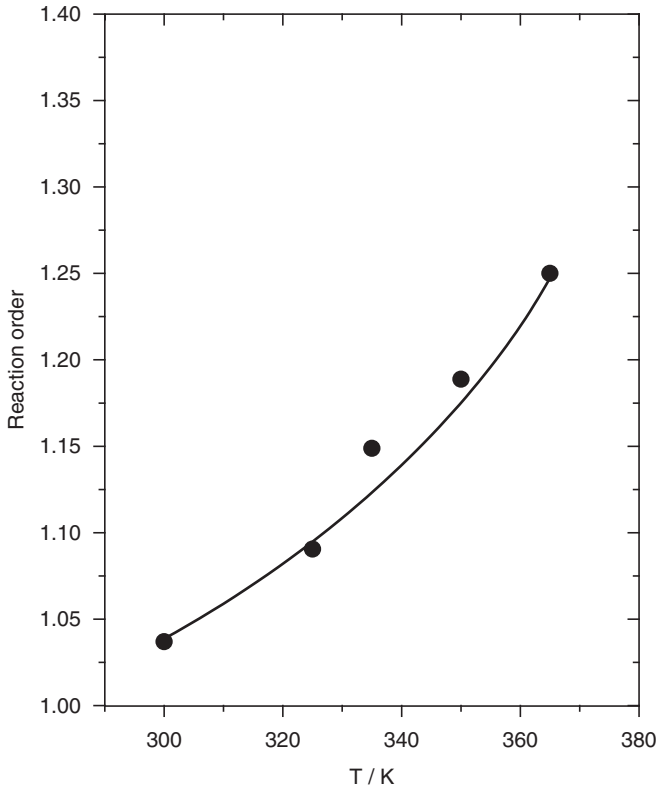

Fig. 1.10 Reaction order in hydrogen for acetylene hydrogenation catalyzed by palladium as a function of reaction temperature. (Reprinted from [88] with permission from Elsevier.)

the conversion kinetics of vinylidene to ethylidene, γ should depend on temperature; therefore, the reaction order should also be temperature-dependent. There has been some suggestion in the literature that indeed the hydrogen reaction order depends on temperature [70–80] and Fig. 1.10 shows the results for acetylene hydrogenation catalyzed by a Pd(111) single crystal [88].

Figure 1.10 shows the plot of the reaction order in hydrogen versus reaction temperature and reveals that the reaction order varies between 1.03 at 300 K to 1.25 at 365 K. This data can be converted into values of γ versus temperature using (1.3); a plot of $\ln(\gamma)$ versus $1/T$ is linear with a slope corresponding to an energy of 4.3 ± 0.2 kcal/mol. These results emphasize the complexity of apparently simple hydrogenation reactions, where the reaction kinetics are not only controlled by the elementary reaction steps on the surface but also by the presence of strongly bound carbonaceous layers. Thus, in order to rationalize the observed catalytic reaction kinetics and to obtain a fundamental, molecular level understanding of the experimentally measured kinetics and thereby fully understand the catalytic reaction pathway, it is sufficient not only to follow the reaction under ultrahigh vacuum conditions, although this is indeed a prerequisite for a full understanding, but also to understand the nature of the surface and how this varies under high reactant pressures [100–102].

1.4.2 Ethylene Hydrogenation

There are clear similarities between palladium-catalyzed acetylene and ethylene hydrogenation since both occur in the presence of a relatively unreactive carbonaceous overlayer. In the case of acetylene hydrogenation, this is a combined ethylidyne and vinylidene layer while in the case of ethylene hydrogenation this consists of only ethylidyne species. Since ethylidyne species are removed by high pressures of hydrogen (see Fig. 1.7), the general picture can therefore be expected to be similar to ethylene hydrogenation where, in this case, a more open surface is formed by ethylidyne removal.

Ethylene adsorbs above a bridge site on Pd(111) at low temperatures in ultrahigh vacuum with the carbon–carbon bond parallel to the surface with a bond length of ~1.42 Å, as depicted in Fig. 1.11, which shows the structure determined from LEED I/E measurements [103]. As noted above, adsorption at room temperature results in the formation of ethylidyne species with a carbon–carbon bond length of ~1.32 Å, located above a threefold hollow site also depicted in Fig. 1.11, again determined using LEED.

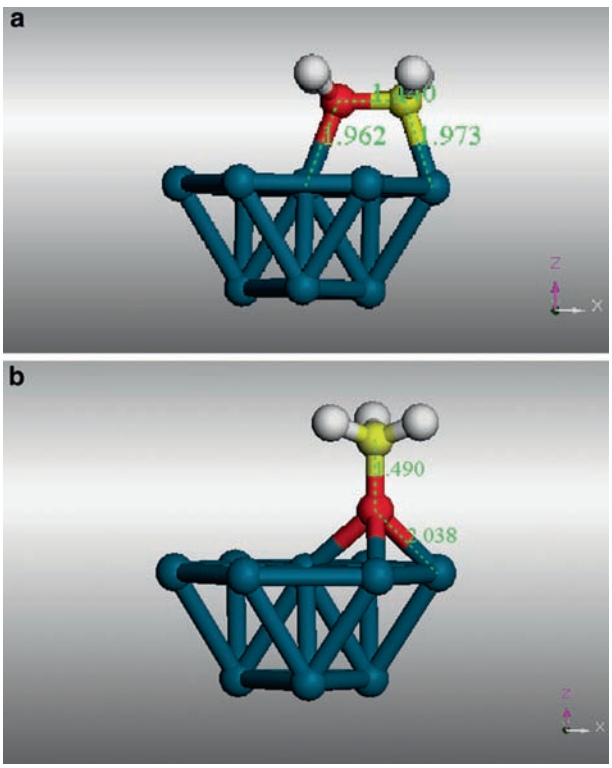

Fig. 1.11 Depiction of di-σ-bonded ethylene and ethylidyne species on Pd(111). (Reprinted from [103] with permission from Elsevier.)

A small amount of ethane is detected in TPD following ethylene adsorption on a hydrogen-covered Pd(111) surface. In this case, a sequential addition of hydrogen according to a Horiuti–Polanyi pathway forms an ethyl intermediate and grafting this onto Pd(111) from ethyl iodide reveals that the addition of the first hydrogen to form an ethyl species is the rate-limiting step [104]. The overall picture appears to be similar to acetylene hydrogenation where the surface is covered by a strongly bound (in this case, ethylidyne) species and the reaction occurs in the presence of ethylidyne which is removed from the surface by hydrogen (Fig. 1.7).

The situation is, more complex since co-adsorbed hydrogen also affects the adsorption state of ethylene as illustrated by the data of Fig. 1.12. This displays the ethylene TPD traces collected following the adsorption of ethylene on hydrogen-covered Pd(111). The strong bonding on the clean surface is indicative of di-σ-bonded ethylene shown in Fig. 1.11, while the decrease in desorption temperature with increasing hydrogen coverage reveals the formation of more weakly π-bonded ethylene. The different forms of ethylene can be distinguished by infrared spectroscopy. Figure 1.13 shows the infrared spectra of ethylene adsorbed on hydrogen-covered surfaces, again measured as a function of hydrogen coverage. This shows that the feature at ~1100 cm^{-1} due to di-σ-bonded ethylene decreases in intensity as the hydrogen coverage increases, while the peak due to π-bonded ethylene at ~930 cm^{-1} increases in intensity with increasing hydrogen coverage, in accordance with the data displayed in Fig. 1.12. The situation for ethylene hydrogenation is

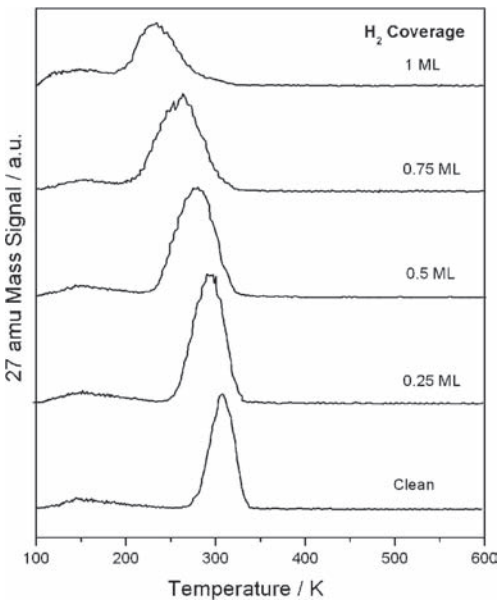

Fig. 1.12 Temperature-programmed desorption spectra of ethylene (0.5 L) on hydrogen-covered Pd(111) as a function of hydrogen coverage. (Reprinted from [101] with permission from Elsevier.)

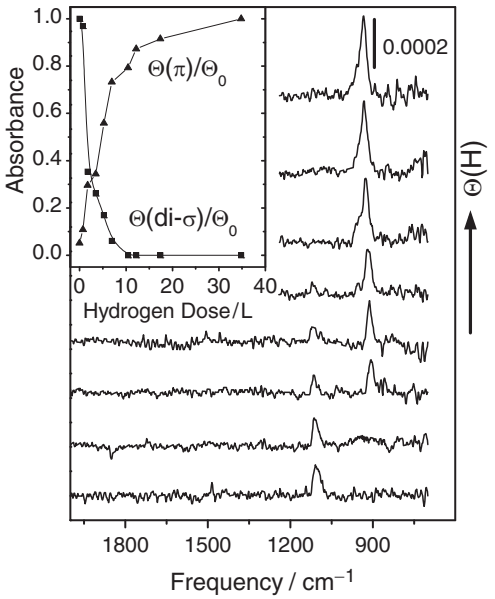

Fig. 1.13 Infrared spectra of ethylene (4 L) on Pd(111) as a function of hydrogen coverage. (Reprinted from [101] with permission from Elsevier.)

even more complex than for acetylene hydrogenation since adsorbed hydrogen weakens the adsorption of ethylene to form π-bonded species.

Hydrogen can adsorb both on top and below the surface on Pd(111) [105–108] where the proportion can be varied by changing the adsorption temperature. By examining the coverage of π- and di-σ-bonded ethylene as a function of the proportion of surface and subsurface hydrogen, it is possible to show that rehybridization is caused exclusively by the presence of subsurface hydrogen [109].

The kinetics of ethylene hydrogenation catalyzed by a Pd(111) single crystal model catalyst have been measured using a high-pressure reactor incorporated into an ultrahigh vacuum chamber [110] where the hydrogenation rate (in units of reactions/site/s) is given by:

$$\text{Rate} = 3.0 \times 10^{-3} P\left(\text{H}_2\right)^n P\left(\text{C}_2\text{H}_4\right)^{-0.6\pm0.1} \exp\left(-10600 \pm 300 / RT\right) \qquad (1.4)$$

and is again typical of noble metal catalyzed hydrogenation reactions [77–80] so that the clean metal sample provides a good model for the working catalyst.

Note that both carbon monoxide and ethylene can adsorb onto ethylidyne-covered Pd(111) [111, 112]. It has been shown above that ethylidyne adsorbed on Pd(111) can react with hydrogen at high pressures [20, 113] so that a similar situation occurs for ethylene hydrogenation as for acetylene hydrogenation. The data of Fig. 1.7 show the rate of ethylidyne removal increases linearly with hydrogen pressure. It is therefore anticipated that the reaction rate will also vary with hydrogen pressure as shown in (1.4). This can be confirmed directly by plotting the ethylene

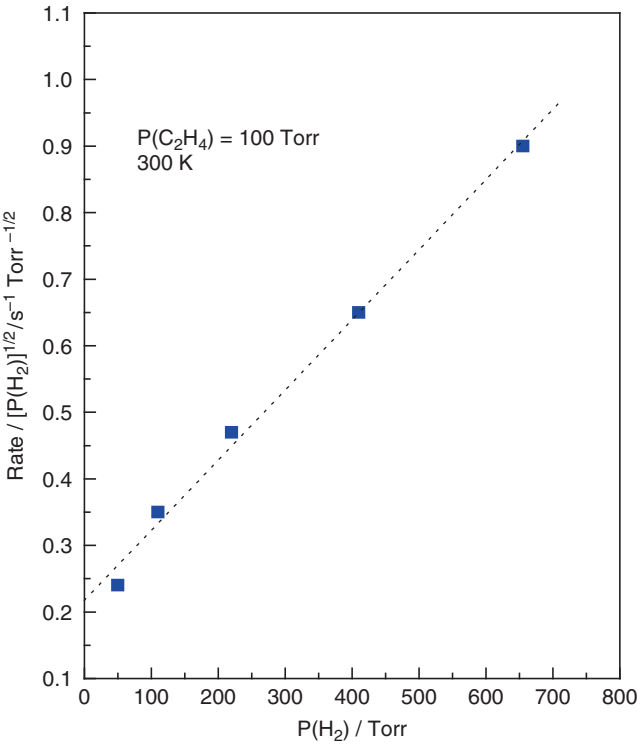

Fig. 1.14 Plot of Rateβ/$\sqrt{P}(H_2)$ versus $P(H_2)$ for ethylene hydrogenation on a palladium foil. (Reprinted from [102] with permission from Elsevier.)

hydrogenation rate/$\sqrt{P}(H)_2$ versus $P(H)_2$. These results are displayed in Fig. 1.14 and show the equation is obeyed by the experimental kinetic data.

The general picture for ethylene hydrogenation is similar to that found for acetylene hydrogenation, where the measured reaction kinetics can only be fully understood by including effects due to the participation of the ethylidyne overlayer. While this hydrogenates much more slowly than adsorbed ethylene and so only contributes in a minor way to the reaction products, its presence on the surface does substantially affect the reaction kinetics.

1.5 Summary

It has been shown that detailed, molecular-level reaction mechanisms can be obtained for catalytic reactions by a combination of surface analyses carried out in ultrahigh vacuum combined with experiments carried out under higher pressures. This approach is illustrated for relatively simple catalytic reactions that occur on

metal single crystals that mimic the working catalyst for which the elementary steps of the reaction occur in ultrahigh vacuum. The results reveal the surface reaction pathways for apparently relatively simple hydrogenation and cyclotrimerization reactions can be quite complex. In particular, rather than occurring on the clean surface, reaction proceeds on a rather dynamic surface whose nature varies with reaction conditions. Clearly, in order for a catalyst to be active for hydrogenation reactions, it must be capable of cleaving hydrogen–hydrogen bonds. This in turn suggests that, as found experimentally, it is also capable of cleaving carbon–hydrogen bonds, resulting in the formation of stable and therefore unreactive ethylidyne and vinylidene species. Alkenes and alkynes can still adsorb onto the surface in the presence of these overlayers but the repulsive interactions between the strongly bound layers and the reactant hydrocarbons lowers the heats of adsorption of the reactants and prevents further decomposition. That is, in the ideal case the surface responds to the reactive environment to passivate itself to allow the reaction to proceed. Furthermore, fully understanding the rather complex catalytic kinetics for apparently rather simple catalytic reactions requires a complete understanding of the chemistry of these strongly bound layers in order to account for the experimentally measured reaction kinetics.

Acknowledgments We gratefully acknowledge support of this work by the United States Department of Energy under several grants and the numerous students and postdoctoral scientists who have worked on these projects.

References

1. Somorjai GA (1996) Modern surface science and surface technologies: an introduction. Chem Rev 96:1223
2. Somorjai GA (1992) The frontiers of surface-structure analysis. Surf Interface Anal 19:493
3. Somorjai GA, McCrea KR (2000) Sum frequency generation: Surface vibrational spectroscopy studies of catalytic reactions on metal single-crystal surfaces. Adv Catal 45:385
4. Davis SM, Zaera F, Somorjai GA (1982) Surface structure and temperature dependence of light-alkane skeletal rearrangement reactions catalyzed over platinum single-crystal surfaces. J Am Chem Soc 104:7453
5. Yang M, Somorjai GA (2004) Adsorption and reactions of C_6 hydrocarbons at high pressures on Pt(111) single-crystal surfaces studied by sum frequency generation vibrational spectroscopy: mechanisms of isomerization and dehydrocyclization of n-hexane. J Am Chem Soc 126:7698
6. Bonivardi AL, Ribeiro FH, Somorjai GA (1996) Turnover rate enhancement of reforming reactions on polycrystalline Pt-Ir foils. J Catal 160:269
7. Yang M, Somorjai GA (2003) Evidence for cyclohexyl as a reactive surface intermediate during high-pressure cyclohexane catalytic reactions on Pt(111) by sum frequency generation vibrational spectroscopy. J Am Chem Soc 125:11131
8. Fujikawa T, Ribeiro FH, Somorjai GA (1998) The effect of Sn on the reactions of n-hexane and cyclohexane over polycrystalline Pt foils. J Catal 178:58
9. Zaera F (2002) Selectivity in hydrocarbon catalytic reforming: a surface chemistry perspective. Appl Catal A 229:75

10. Tjandra S, Zaera F (1996) A surface science study of the hydrogenation and dehydrogenation steps in the interconversion of C_6 cyclic hydrocarbons on Ni(100). J Catal 164:82
11. Marsh AL, Somorjai GA (2005) Structure, reactivity, and mobility of carbonaceous overlayers during olefin hydrogenation on platinum and rhodium single crystal surfaces. Top Catal 34:121
12. Zaera F, Somorjai GA (1984) Hydrogenation of ethylene over platinum (111) single-crystal surfaces. J Am Chem Soc 106:2288
13. Kaltchev M, Thompson AW, Tysoe WT (1997) Reflection-absorption infrared spectroscopy of ethylene on palladium(111) at high pressure. Surf Sci 391:145
14. Koestner RJ, Van Hove MA, Somorjai GA (1983) Molecular structure of hydrocarbon monolayers on metal surfaces. J Phys Chem 87:203
15. Kesmodel LL, Dubois LH, Somorjai GA (1978) Dynamical LEED study of C_2H_2 and C_2H_4 chemisorption on Pt(111): evidence for the ethylidyne CH_3-C group. Chem Phys Lett 56:267
16. Cremer P, Stanners C, Neimantsverdreit J, Shen Y, Somorjai GA (1995) The conversion of di-sigma bonded ethylene to ethylidyne on Pt(111) monitored with sum-frequency generation – evidence for an ethylidene (or ethyl) intermediate. Surf Sci 328:111
17. Cremer P, Somorjai GA (1995) Surface science and catalysis of ethylene hydrogenation. J Chem Soc Faraday Trans 91:3671
18. Cremer P, Su X, Shen Y, Somorjai GA (1996) Ethylene hydrogenation on Pt(111) monitored in situ at high pressures using sum frequency generation. J Am Chem Soc 118:2942
19. Cremer P, Su X, Shen Y, Somorjai GA (1996) The first measurement of an absolute surface concentration of reaction intermediates in ethylene hydrogenation. Catal Lett 40:143
20. Beebe TP Jr, Yates JT Jr (1986) An in situ infrared spectroscopic investigation of the role of ethylidyne in the ethylene hydrogenation reaction on palladium/alumina. J Am Chem Soc 108:663
21. Beebe TP Jr, Albert MR, Yates JT Jr (1986) Infrared spectroscopic observation and characterization of surface ethylidyne on supported palladium on alumina. J Catal 96:1
22. Chesters MA, McCash EM (1987) Ethylidyne formation on Pt(111), studied by FT-RAIRS. Surf Sci 187:L639
23. Mousin SB, Trenary M, Robota HJ (1989) Kinetics of ethylidyne formation on Pt(111) from time-dependent infrared-spectroscopy. Chem Phys Lett 154:511
24. Ma Z, Zaera F (2006) Organic chemistry on solid surfaces. Surf Sci Rep 61:229
25. Bent BE (1996) Mimicking aspects of heterogeneous catalysis: generating, isolating, and reacting proposed surface intermediates on single crystals in vacuum. Chem Rev 96:1361
26. Zaera F (1994) Molecular approach to the study of the mechanisms of alkyl reactions on metal surfaces. J Mol Catal 86:221
27. Zaera F (1992) Preparation and reactivity of alkyl groups adsorbed on metal surfaces. Acc Chem Res 25:260
28. Zaera F (1995) An organometallic guide to the chemistry of hydrocarbon moieties on transition metal surfaces. Chem Rev 95:2651
29. Horiuti J, Polanyi M (1930) Exchange reactions of hydrogen on metallic catalysts. Trans Faraday Soc 30:1164
30. Horiuti J (1948) Hydrogen addition on metal catalysts. Catalyst 2:1
31. Tysoe WT, Nyberg GL, Lambert RM (1983) Photoelectron spectroscopy and heterogeneous catalysis: benzene and ethylene from acetylene on Pd(111). Surf Sci 135:128
32. Sesselman W, Woratschek B, Ertl G, Küppers J, Haberland H (1983) Low-temperature formation of benzene from acetylene on a Pd(111) surface. Surf Sci 130:245
33. Gentle TM, Muetterties EL (1983) Acetylene, ethylene, and arene chemistry of palladium surfaces. J Phys Chem 87:2469
34. Tysoe WT, Nyberg GL, Lambert RM (1983) Low temperature catalytic chemistry of the Pd(111) surface: benzene and ethylene from acetylene. J Chem Soc Chem Commun 623.
35. Avery NA (1985) Adsorption and reactivity of acetylene on a Copper (110) surface. J Am Chem Soc 107:6711
36. Xu C, Peck JW, Koel BE (1993) A new catalyst for benzene production from acetylene under UHV conditions – Sn/Pt(111) surface alloys. J Am Chem Soc 115:751

37. Badderley CJ, Ormerod RM, Stephenson AW, Lambert RM (1995) Surface-structure and reactivity in the cyclization of acetylene to benzene with Pd overlayers and Pd/Au surface alloys on Au(111). J Phys Chem 99:5146
38. Pierce KG, Barteau MA (1993) Cyclotrimerization of alkynes on reduced TiO_2(001) surfaces. J Phys Chem 115:751
39. Rucker TG, Logan MA, Muetterties EM, Somorjai GA (1986) Conversion of acetylene to benzene over palladium single-crystal surfaces. 1. The low-pressure stoichiometric and the high-pressure catalytic reactions. J Phys Chem 90:2703
40. Ramirez-Cuesta A, Valladares D, Velasco A, Zgrablich G, Tysoe WT, Ormerod RM, Lambert RM (1993) Desorption of benzene from Pd(111): A simulation study. J Phys: Condens Matter 5:A137
41. Hoffmann H, Zaera F, Ormerod RM, Lambert RM, Wang LP, Tysoe WT (1990) Discovery of a tilted form of benzene chemisorbed on Pd(111): A NEXAFS and photoemission investigation. Surf Sci 232:259
42. Patterson CH, Lambert RM (1998) Molecular pathways in the cyclotrimerization of ethyne on palladium: Role of the C_4 intermediate. J Am Chem Soc 110:6871
43. Ormerod RM, Lambert RM, Hoffmann H, Zaera F, Yao JM, Saldin DK, Wang LP, Bennett DW, Tysoe WT (1993) NEXAFS identification of a catalytic reaction intermediate: C_4H_4 on Pd(111). Surf Sci 295:277
44. Ramirez-Cuesta AJ, Zgrablich G, Tysoe WT (1995) Simulation of benzene formation from acetylene on palladium and oxygen-covered palladium surfaces. Surf Sci 340:109
45. Inoue Y, Kojima I, Moriki S, Yasumori I (1976) Template effects in palladium catalysis. In: Proceedings of the sixth international congress on catalysis, vol 1, p 139
46. Abdelrehim IM, Caldwell TE, Land DP (1996) Coverage effects on the kinetics of benzene formation from acetylene on Pd(111): A laser-induced thermal desorption Fourier transform mass spectrometry investigation. J Phys Chem 100:10265
47. Abdelrehim IM, Thornburg NA, Sloan JT, Caldwell TE, Land DP (1995) Kinetics and mechanism of benzene formation from acetylene on Pd(111) studied by laser-induced thermal-desorption Fourier-transform mass-spectrometry. J Am Chem Soc 117:9509
48. Abdelrehim IM, Thornburg NA, Sloan JT, Land DP (1993) Benzene and thiophene formation from acetylene on sulfided Pd(111) studied by LITD FTMS. Surf Sci 298:L169
49. Janssens TVW, Völkening S, Zambelli T, Winterlin J (1998) Direct observation of surface reactions of acetylene on Pd(111) with scanning tunneling microscopy. J Phys Chem 102:6251
50. Ormerod RM, Lambert RM (1990) Heterogeneously catalyzed cyclotrimerization of ethyne to benzene over supported palladium catalysts. J Chem Soc Chem Commun 20:1421
51. Ormerod RM, Lambert RM, Hoffmann H, Zaera F, Wang LP, Bennett DW, Tysoe WT (1994) Room temperature chemistry of acetylene on Pd(111): formation of vinylidene. J Phys Chem 98:2134
52. Ormerod RM, Lambert RM, Bennett DW, Tysoe WT (1995) Temperature programmed desorption of co-adsorbed hydrogen and acetylene on Pd(111). Surf Sci 330:1
53. Zheng T, Tysoe WT, Poon HC, Saldin DK (2003) Structural determination of ordered and disordered organic molecules on a surface from the substrate diffraction spots in low energy electron diffraction: $(\sqrt{3}\times\sqrt{3})R30°$-$C_2H_2$ and disordered CH_3OH on Pd(111). Surf Sci 543:19
54. Sellers H (1990) Structures and vibrational frequencies of acetylene in 3 binding sites on the Pd(111) surface. J Phys Chem 94:8329
55. Pallassana V, Neurock M, Lusvardi VS, Lerov JJ, Kragten DD, van Santen RA (2002) A density functional theory analysis of the reaction pathways and intermediates for ethylene dehydrogenation over Pd(111). J Phys Chem B 106:1659
56. Clotet A, Ricart JM, Pacchioni G (1998) Bonding of vinylidene on Pd(111). J Mol Struct 458:123
57. Somorjai GA (1996) The flexible surface: new techniques for molecular level studies of time dependent changes in metal surface structure and adsorbate structure during catalytic reactions. J Mol Catal A: Chem 107:39
58. Stacchiola D, Wu G, Kaltchev M, Tysoe WT (2001) Molecular beam and infrared spectroscopic studies of the thermodynamics of CO on clean and vinylidene-covered Pd(111). J Chem Phys 115:3315

59. Conrad H, Ertl G, Koch J, Latta EE (1974) Adsorption of CO on Pd single crystal surfaces. Surf Sci 43:462
60. Ertl G, Koch J (1970) Adsorption von CO auf einer Palladium(111)-Oberfläche. Z Naturforsch A: Phys Sci 25:1906
61. Colthup NB, Daly LH, Wiberley SE (1964) Infrared and Raman spectroscopy. Academic Press, New York
62. Ormerod RM, Lambert RM (1992) Critical ensemble required for acetylene cyclization on Pd(111) - A study of steric inhibition by coadsorbed oxygen. J Phys Chem 96:8111
63. Baddeley CJ, Tikhov M, Hardacre C, Lomas JR, Lambert RM (1996) Ensemble effects in the coupling of acetylene to benzene on a bimetallic surface: a study with Pd{111}/Au. J Phys Chem 100:2189
64. Beckhaus R (1997) Carbenoid complexes of electron-deficient transition metals – Syntheses of and with short-lived building blocks. Angew Chem Int Ed 36:687
65. Beckhaus R, Oster J, Ganter B, Englert U (1997) Vinyltitanium complexes containing the [2-(N,N-dimethylamino)ethyl]tetramethylcyclopentadienyl ligand Cp-*N. Generation and reactivity of the vinylidene intermediate [(Cp-*N)(Cp*)Ti=C=CH_2] (Cp-*N=eta(5)-$C_5Me_4(CH_2)(2)NMe_2$, Cp*=eta(5)-C_5Me_5). Organometallics 16:3902
66. Beckhaus R, Sang J, Wagner T, Ganter B (1996) Reactivity of acetylenes toward the titanocene vinylidene fragment [Cp^*_2Ti=C=CH_2]. Formation of methylenetitanacyclobutenes and vinyltitanium acetylides. Crystal and molecular structures of Cp^*_2TiCR'=CR''C=CH_2 (R'=R''=CH_3; R'=SiMe(3), R''=C_6H_5) and Cp^*_2Ti(CH=CH_2)(C CPh). Organometallics 15:1176
67. Levy GC, Lichter RL, Nelson GL (1980) Carbon-13 Nuclear Magnetic Resonance Spectroscopy. Wiley Interscience, New York
68. Kaltchev M, Molero H, Stacchiola D, Wu G, Blumenfeld A, Tysoe WT (1999) On the reaction pathway for the formation of benzene from acetylene catalyzed by palladium. Catal Lett 60:11
69. Stacchiola D, Wu G, Molero H, Tysoe WT (2001) On the effect of hydrogen on the palladium-catalyzed formation of benzene from acetylene. Catal Lett 71:1
70. Bond GC, Wells PB (1965) The hydrogenation of acetylene: II. The reaction of acetylene with hydrogen catalyzed by alumina-supported palladium. J Catal 5:65
71. Bond GC, Wells PB (1965) The hydrogenation of acetylene: I. The reaction of acetylene with hydrogen catalyzed by alumina-supported platinum. J Catal 4:211
72. Yasunobi T, Yasumori I (1971) Pressure jump and isotope replacement studies of acetylene hydrogenation on palladium surface. J Phys Chem 75:880
73. Moses JM, Weiss AH, Matusek K, Guczi L (1984) The effect of catalyst treatment on the selective hydrogenation of acetylene over palladium/alumina. J Catal 86:417
74. Gua LZ, Kho KE (1988) Kinetics of acetylene hydrogenation on palladium deposited on alumina. Kinet Catal 29:381
75. Moyes RB, Walker DW, Wells PB, Whan DA, Irvine EA (1989) An unusual form of non-Arrhenius behaviour in ethyne hydrogenation over palladium catalysts. Appl Catal 55:L5
76. Adúriz HR, Bodnariuk P, Dennehy M, Grgola CE (1990) Activity and selectivity of Pd/α-Al_2O_3 for ethyne hydrogenation in a large excess of ethene and hydrogen. Appl Catal 58:227
77. Bos ANR, Westerterp K (1978) Mechanism and kinetics of the selective hydrogenation of ethyne and ethene. Chem Eng Process 32:1
78. Bond GC (1962) Catalysis by metals. Academic Press, New York
79. Beeck O (1950) Hydrogenation catalysts. Faraday Discuss 8:118
80. Bond GC, Wells PB (1964) The mechanism of the hydrogenation of unsaturated hydrocarbons on transition metal catalysts. Adv Catal 15:91
81. Wang L, Soto C, Tysoe WT (1993) The kinetics of propylene metathesis catalyzed by a molybdenum (100) single crystal. J Catal 143:92
82. Bartlett BF, Molero H, Tysoe WT (1997) The metathesis of propylene catalyzed by model oxides studied using a high-pressure reactor incorporated into an ultrahigh vacuum chamber. J Catal 167:470
83. Wu G, Kaltchev M, Tysoe WT (1999) The kinetics and infrared spectroscopy of C_1 hydrocarbons adsorbed on clean and oxygen-modified Mo(100). Surf Rev Lett 6:13

84. Borodzinski A, Bond GC (2006) Selective hydrogenation of ethyne in ethene-rich streams on palladium catalysts. Part 1. Effect of changes to the catalyst during reaction. Catal Rev – Sci Eng 48:91
85. Tysoe WT, Nyberg GL, Lambert RM (1986) Selective hydrogenation of acetylene over palladium in ultra high vacuum. J Phys Chem 90:3188
86. Azad S, Kaltchev M, Stacchiola D, Wu G, Tysoe WT (2000) On the reaction pathway for the hydrogenation of acetylene and vinylidene on Pd(111). J Phys Chem B 104:3107
87. Goodman DW (1966) Chemical and spectroscopic studies of metal oxide surfaces. J Vac Sci Technol A 14:1526
88. Molero H, Bartlett BF, Tysoe WT (1999) The hydrogenation of acetylene catalyzed by palladium: hydrogen pressure dependence. J Catal 181:49
89. Al-Ammar AS, Webb G (1978) Hydrogenation of acetylene over supported metal catalysts: Part 1 – Adsorption of [^{14}C] Acetylene and [^{14}C] ethylene on silica supported rhodium, iridium and palladium and alumina supported palladium. J Chem Soc Faraday Trans 74:195
90. Al-Ammar AS, Webb G (1979) Hydrogenation of acetylene over supported metal catalysts: Part 3 – [^{14}C] tracer studies of the effect of added ethylene and carbon monoxide on the reaction catalyzed by silica-supported palladium, rhodium and iridium. J Chem Soc Faraday Trans 75:1900
91. McGowan WT, Kemball C, Whan DA, Scurrell MS (1977) Hydrogenation of acetylene in excess ethylene on an alumina supported palladium catalyst in static system. J Chem Soc Faraday Trans 73:632
92. Margitfalvi J, Guczi L, Weiss AH (1981) Reactions of acetylene during hydrogenation on Pd black catalyst. J Catal 72:185
93. Sassen NRM, Den Hartog AJ, Jongerious F, Aarts JFM, Ponec V (1989) Adsorption and reactions of ethyne – Effects of modifiers and formation of bimetallics. Faraday Discuss 87:311
94. Den Hartog AJ, Deng M, Jongerious F, Ponec V (1990) Hydrogenation of acetylene over various group VIII metals – Effect of particle size and carbonaceous deposits. J Mol Catal 60:99
95. Menshikov WA, Falkovitsch JG, Aerov ME (1975) Hydrogenation kinetics of acetylene on a palladium catalyst in the presence of ethylene. Kinet Catal 16:1538
96. Houzvicka J, Pestman R, Ponec V (1995) The role of carbonaceous deposits and support impurities in the selective hydrogenation of ethyne. Catal Lett 30:289
97. Sarkany A, Guczi L, Weiss AH (1984) On the aging phenomena in palladium catalysed acetylene hydrogenation. Appl Catal 10:369
98. LeViness S, Nair V, Weiss AH, Schay Z, Guczi L (1984) Acetylene hydrogenation selectivity control on PdCu/Al_2O_3 catalysts. J Mol Catal 25:131
99. Borodzinski A (1997) A, Golebiowski, Surface heterogeneity of supported palladium catalyst for the hydrogenation of acetylene-ethylene mixtures. Langmuir 13:883
100. Tysoe WT (1999) Palladium-catalyzed acetylene cyclotromerization: from ultrahigh vacuum to high-pressure catalysis. Isr J Chem 38:313
101. Stacchiola D, Calaza F, Zheng T, Tysoe WT (2005) Hydrocarbon conversion on palladium catalysts. J Mol Catal A: Chem 228:35
102. Stacchiola D, Molero H, Tysoe WT (2001) Palladium-catalyzed cyclotrimerization and hydrogenation: from ultrahigh vacuum to high-pressure catalysis. Catal Today 65:3
103. Zheng T, Stacchiola D, Poon HC, Saldin DK, Tysoe WT (2004) Determination of the structure of disordered overlayers of ethylene on clean and hydrogen-covered Pd(111) by low energy electron diffraction. Surf Sci 564:71
104. Stacchiola D, Azad S, Burkholder L, Tysoe WT (2001) An investigation of the reaction pathway for ethylene hydrogenation on Pd(111). J Phys Chem 105:11233
105. Behm H, Christman K, Ertl G (1980) Adsorption of hydrogen on Pd(100). Surf Sci 99:320
106. Conrad H, Ertl G, Latta EE (1974) Adsorption of hydrogen on palladium single crystal surfaces. Surf Sci 41:435
107. Conrad H, Ertl G, Küppers J, Latta EE (1976) Ultraviolet photoelectron spectra from hydrogen adsorbed on Ni(111) and Pd(111) surfaces. Surf Sci 58:578
108. Greuter F, Eberhardt W, DiNardo J, Plummer EW (1981) Bonding to Ni, Pd and Pt: An angle resolved photoemission study. J Vac Sci Technol 18:433

109. Stacchiola D, Tysoe WT (2003) The effect of subsurface hydrogen on the adsorption of ethylene on Pd(111). Surf Sci 540:L600
110. Molero H, Stacchiola D, Tysoe WT (2005) The kinetics of ethylene hydrogenation catalyzed by metallic palladium. Catal Lett 101:145
111. Stacchiola D, Kaltchev M, Tysoe WT (2000) The adsorption and structure of CO on ethylidyne-covered Pd(111). Surf Sci 470:L32
112. Stacchiola D, Tysoe WT (2002) The adsorption of ethylene on ethylidyne-covered Pd(111). Surf Sci 513:L431
113. Davis S, Zaera F, Gordon BE, Somorjai GA (1985) Radiotracer and thermal desorption studies of dehydrogenation and atmospheric hydrogenation of organic fragments obtained from [^{14}C]ethylene chemisorbed over Pt(111) surfaces. J Catal 92:240